Design and Implementation of a Robust Controller for a Free Gyro-Stabilized Mirror System

Boon C. Siew,[1] Ben M. Chen,[1] and Tong H. Lee[1]

In this paper, we consider the problem of designing a robust controller for a multivariable servomechanism of a free gyro-stabilized mirror system where there exists cross-coupling between the axes. The nonlinear dynamics of the system are first linearized and reformulated into an H_∞ problem. A reduced order output feedback controller is then designed using the asymptotic time-scale and eigenstructure assignment (ATEA) technique. The overall design has been implemented using a personal computer with C++ and tested on the actual gyro-stabilized mirror system. Our simulation and implementation results show that the design is very successful.

1 Introduction to the Problem

Electro-optical (E-O) sensors that are mounted on vehicles such as aircraft, helicopter, and tanks are subjected to vibrations introduced by these platforms. These vibrations cause the line-of-sight (LOS) of the E-O sensors to shift, resulting in serious degradation of the image quality (see for example, Bigley and Rizzo, 1987). This problem is even more pronounced in systems with high magnification property. One way of overcoming it is to use free gyro-stabilization. A gyroscope or gyro is basically an axially symmetrical mass rotating under a high constant speed. With the magnitude of the angular inertia and the speed of rotation both kept constant, the momentum generated is also fixed. Bearing in mind that the momentum is a vector quantity, this implies that the directional orientation is maintained. Therefore under the absence of large external forces, a gyro is capable of maintaining the orientation of its spin axis in the inertia space. By choosing an appropriate high value for the speed of rotation, the vibrational torque produced by the platforms can be made insignificant as compared to the momentum generated. The LOS can thus be stabilized by simply designing a system such that the LOS and the gyro's spin axis are parallel in space. However, a spinning gyro has another property known as precession. This means that if a torque is applied to one axis, it will, contrary to the intuitions of mechanics, rotate in the direction of another axis (Perry, 1957). In this paper, we consider a multivariable servomechanism free gyro-stabilized mirror system. More specifically, it is a two-input-two-output system. The control of this multiple-input-multiple-output system is not a simple problem solved by using conventional PID controllers, because there exist cross-coupling interactions between the dynamics of the two axes. In addition, the controller has to maintain stable operation even when there are changes in the system dynamics. Over the years, many researchers have worked on this system, and the control methodologies studied include adaptive with feedforward paradigm (see e.g., Lee et al., 1996, and Yang and Chang, 1996), neural network control (see e.g., Ge et al., 1997), fuzzy logic (see e.g., Lee, 1995), linear quadratic Gaussian technique (see e.g., Bigley and Rizzo, 1997, and Constancis and Sorine, 1992), and feedback linearization (see e.g., Dzielski et al., 1991), to name a few. We tackle in this paper a gyro-stabilized mirror system design using an H_∞ control approach. We will design a simple low order controller such that the overall closed-loop system would have fast tracking and good robustness performance.

2 The Free Gyro-Stabilized Mirror System

Figure 1 is a schematic diagram of the gyro mirror. It consists of the following essential components: (i) a flywheel and its spin motor; (ii) gimbals that provide two degrees of freedom to the flywheel and two torque motors for slewing purposes; and (iii) a mirror that is geared to the gimbals through a 2:1 reduction drive mechanism.

Because no rigid body can spin forever, a piece of a pancake spin motor (flywheel) is used as the gyroscope (gyro). By adjusting the input torque, the flywheel can be made to spin at a high constant velocity about its spin *axis* (Axis 3 in Fig. 1). The flywheel is mounted on an inner gimbal so that it can rotate freely up and down. This axis of rotation is called the pitch axis and corresponds to Axis 2 in Fig. 1. The inner gimbal is in turn mounted on an outer gimbal, which provides another axis of freedom (the yaw axis or Axis 1) which moves left and right. Note that with these three axes being orthogonal to each other, the system's line-of-sight (LOS) can be made parallel to Axis 3 by aligning the mirror axis to the pitch axis.

A torque motor is attached to each of the inner and outer gimbals. These torque motors move the gyro either in the yaw or in the pitch direction, and are thus named the yaw and the pitch motors, respectively. Providing appropriate torque through these motors causes the system to precess relative to the inertia space to achieve some desired line-of-sight (LOS). Removing these input torques stabilizes the LOS in its new position. The angular positions about which the yaw and the pitch axes are defined as θ_1 and θ_2, respectively. θ_1 and θ_2 can be measured through potentiometers mounted on the inner and outer gimbals. There are, however, no velocity sensors to sense $\dot\theta_1$ and $\dot\theta_2$. Due to physical constraints, the workspace for the gyro-stabilized mirror is limited to $-50° \le \theta_1 \le 50°$ and $-30° \le \theta_2 \le 30°$. Also, the maximum torques for both yaw and pitch motors are physically limited to a range from -0.5 Nm to 0.5 Nm.

In this particular system considered here, a mirror is used in

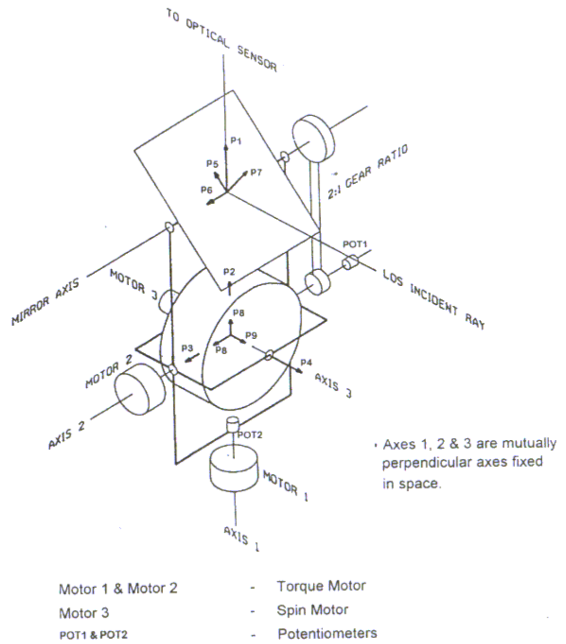

Fig. 1 Schematic diagram of the gyro mirror

[1] Department of Electrical Engineering, National University of Singapore, Singapore 119260.

Contributed by the Dynamic Systems and Control Division of THE AMERICAN SOCIETY OF MECHANICAL ENGINEERS. Manuscript received by the Dynamic Systems and Control Division March 12, 1998. Associate Technical Editor: T. Kurfess.

place of the actual electro-optical (E-O) sensors. The advantage of doing this is that the E-O sensors will not form an integral part of the system. Therefore any E-O sensor can be used without affecting the system's dynamics. The mirror is connected to the flywheel-gimbal structure via a 2:1 reduction drive. This 2:1 reduction drive is required because when the mirror is tilted by an angle α, the reflected LOS is rotated by 2α.

Ng (1986) developed the dynamical equations of the gyro mirror by applying the Lagrange's method. The equations are:

$$M_1(\theta)\ddot{\theta}_1 + H_1(\theta, \dot{\theta}) + G_1(\theta, \dot{\theta}, \dot{\theta}_3) = u_1, \tag{1}$$

$$M_2(\theta)\ddot{\theta}_2 + H_2(\theta, \dot{\theta}) + G_2(\theta, \dot{\theta}, \dot{\theta}_3) = u_2, \tag{2}$$

where $\theta = (\theta_1, \theta_2)'$; u_1 and u_2 are the actuator torques for the yaw and the pitch axes; $\dot{\theta}_3$ is the spin velocity of the flywheel. The parameters in Eqs. (1)–(2) are defined as follows:

$$M_1 = \bar{a} + \bar{d} + (\bar{b} - \bar{d} + \bar{l}) \cos^2 \theta_2 + \tfrac{1}{2}(\bar{e} + \bar{g}) + \tfrac{1}{2}(\bar{e} - \bar{g}) \sin \theta_2, \tag{3}$$

$$H_1 = -(\bar{b} - \bar{d} + \bar{l})\dot{\theta}_1\dot{\theta}_2 \sin 2\theta_2 + \tfrac{1}{2}(\bar{e} - \bar{g})\dot{\theta}_1\dot{\theta}_2 \cos \theta_2 + \bar{k}\dot{\theta}_1\dot{\theta}_2 \sin \theta_2 \cos \theta_2, \tag{4}$$

$$G_1 = \bar{k}\dot{\theta}_2\dot{\theta}_3 \cos \theta_2, \tag{5}$$

$$M_2 = \bar{c} + \frac{\bar{f}}{4} + \bar{l}, \tag{6}$$

$$H_2 = \tfrac{1}{2}(\bar{b} - \bar{d} + \bar{l})\dot{\theta}_1^2 \sin 2\theta_2 - \tfrac{1}{4}(\bar{e} - \bar{g})\dot{\theta}_1^2 \cos \theta_2 - \bar{k}\dot{\theta}_1^2 \sin \theta_2 \cos \theta_2, \tag{7}$$

$$G_2 = -\bar{k}\dot{\theta}_1\dot{\theta}_3 \cos \theta_2, \tag{8}$$

where $\bar{a}$, $\bar{b}$, $\bar{c}$, $\bar{d}$, $\bar{e}$, $\bar{f}$, $\bar{g}$, $\bar{l}$, and $\bar{k}$ are all physical constants representing the various moment of the inertia of the system. Ng (1986) and Lee (1995) identified these constants, which have the following values:

$$\bar{a} = 0.004, \quad \bar{b} = 0.00128, \quad \bar{c} = 0.00098, \quad \bar{d} = 0.02, \tag{9}$$

and

$$\bar{e} = 0.0049, \quad \bar{f} = 0.0025, \quad \bar{g} = 0.00125,$$

$$\bar{l} = 0.0032, \quad \bar{k} = 0.0025. \tag{10}$$

The above parameters have units of kg $\cdot$ m^2. As can be seen from the above equations, the system is highly nonlinear and there exist cross-coupling terms between the yaw and the pitch axes. When spin velocity ($\dot{\theta}_3$) is large, the interactions are acting mainly through the G_1 and G_2 terms.

3 Controller Design Using H_∞ Disturbance Decoupling Approach

In this section, we will briefly revisit the well-known problem of H_∞ almost disturbance decoupling. We will then use it to solve our gyro-stabilized mirror targeting control system design problem. We consider the problem of H_∞ almost disturbance decoupling with measurement feedback and with internal stability (H_∞-ADDPMS) for the following continuous-time linear system:

$$\Sigma : \begin{cases} \dot{x} = A\,x + B\,u + E\,w, \\ y = C_1\,x + D_1\,w, \\ h = C_2\,x + D_2\,u, \end{cases} \tag{11}$$

where $x \in \mathbb{R}^n$ is the vector of states, $u \in \mathbb{R}^m$ is the vector of control inputs, $y \in \mathbb{R}^l$ is the vector of measurements, $w \in \mathbb{R}^q$ is the vector of disturbances, and $h \in \mathbb{R}^p$ is the vector of outputs to be controlled. A, B, E, C_1, C_2, D_1, and D_2 are constant matrices of appropriate dimensions. We define Σ_P to be the subsystem characterized by the matrix quadruple (A, B, C_2, D_2) and Σ_Q to be the subsystem characterized by the matrix quadruple (A, E, C_1, D_1). The following dynamic feedback control laws are investigated:

$$\Sigma_c : \begin{cases} \dot{x}_c = A_c\,x_c + B_c\,y, \\ u = C_c\,x_c + D_c\,y. \end{cases} \tag{12}$$

The controller Σ_c of (12) is said to be internally stabilizing when applied to the system Σ, if the following matrix is asymptotically stable:

$$A_{\mathrm{cl}} := \begin{bmatrix} A + BD_cC_1 & BC_c \\ B_cC_1 & A_c \end{bmatrix}, \tag{13}$$

i.e., all its eigenvalues lie in the open left-half complex plane. Denote by T_{hw} the corresponding closed-loop transfer matrix from the disturbance w to the output to be controlled h, i.e.,

$$T_{hw} = D_2D_cD_1 + [C_2 + D_2D_cC_1 \quad D_2C_c] \times \left(sI - \begin{bmatrix} A + BD_cC_1 & BC_c \\ B_cC_1 & A_c \end{bmatrix}\right)^{-1} \begin{bmatrix} E + BD_cD_1 \\ B_cD_1 \end{bmatrix} \tag{14}$$

The H_∞ norm of the transfer matrix T_{hw} is given by

$$\|T_{hw}\|_\infty := \sup_{\omega \in [0,\infty)} \sigma_{\max}[T_{hw}(j\omega)], \tag{15}$$

where $\sigma_{\max}[\,\cdot\,]$ denotes the largest singular value. Then the H_∞-ADDPMS can be formally defined as follows.

Definition 3.1. The H_∞ almost disturbance decoupling problem with measurement feedback and with internal stability (H_∞-ADDPMS) for Σ of (11) is said to be solvable if, there exists a parameterized controller, with a parameter say ϵ, of the form (12) such that as $\epsilon \to 0$ (i) the closed-loop system comprising the system (11) and the controller (12) is asymptotically stable, and (ii) the H_∞-norm of the closed-loop transfer matrix from the disturbance w to the controlled output h tends to 0, i.e., $\|T_{hw}\|_\infty \to 0$.

It turns out (see, for example, Chen et al., 1998) that the H_∞-ADDPMS for the given system Σ is always solvable if 1) the subsystem Σ_P is right invertible and of minimum phase, and 2) the subsystem Σ_Q is left invertible and of minimum phase. As it will be seen shortly, our gyro-stabilized mirror targeting system will satisfy these conditions. Thus, we will recall in the following a simplified version of the asymptotic time-scale and eigenstructure assignment (ATEA) method from Chen et al. (1998), which solves the H_∞-ADDPMS for a given Σ whose subsystems satisfy the above two conditions. Moreover, the ATEA design method has the capability of assigning appropriate eigenstructures such that the resulting closed-loop system has zero overshoot in its step response. The detailed proofs of the algorithm can be found in Chen et al. (1998) and Chen (1998).

Stage 1. The following is the ATEA algorithm for constructing a parameterized state feedback gain $F(\epsilon)$ such that $u = F(\epsilon)x$ will solve the problem of disturbance decoupling with internal stability for the system of (11) with $C_1 = I$ and $D_1 = 0$. In this case, the system representation is

$$\Sigma : \begin{cases} \dot{x} = A\,x + B\,u + E\,w, \\ y = x \\ h = C_2\,x + D_2\,u, \end{cases} \tag{16}$$

where (A, B, C_2, D_2) or Σ_P is assumed to be right invertible and of minimum phase.

Step S.F.1: Utilize the results of the special coordinate basis of linear systems of Sannuti and Saberi (1987), and Saberi and Sannuti (1990) (see also Chen, 1998, for the detailed proofs of its properties), to find nonsingular state, input and output transformations Γ_s, Γ_i, and Γ_o to the system (16) such that if we let

$$x = \Gamma_s\tilde{x}, \quad h = \Gamma_o\tilde{h}, \quad u = \Gamma_i\tilde{u}, \tag{17}$$

we will have

$$\tilde{x} = \begin{pmatrix} x_a^- \\ x_c \\ x_d \end{pmatrix}, \quad x_d = \begin{pmatrix} x_1 \\ x_2 \\ \vdots \\ x_{m_d} \end{pmatrix}, \tag{18}$$

$$\tilde{h} = \begin{pmatrix} h_0 \\ h_d \end{pmatrix}, \quad h_d = \begin{pmatrix} h_1 \\ h_2 \\ \vdots \\ h_{m_d} \end{pmatrix}, \quad \tilde{u} = \begin{pmatrix} u_0 \\ u_d \\ u_c \end{pmatrix}, \quad u_d = \begin{pmatrix} u_1 \\ u_2 \\ \vdots \\ u_{m_d} \end{pmatrix}, \tag{19}$$

and

$$\dot{x}_a^- = A_{aa}^- x_a^- + B_{0a}^- h_0 + L_{ad}^- h_d + E_a^- w, \tag{20}$$

$$\dot{x}_c = A_{cc} x_c + B_{0c} h_0 + L_{cd} h_d + B_c E_{ca}^- x_a^- + B_c u_c + E_c w, \tag{21}$$

$$h_0 = C_{0a}^- x_a^- + C_{0c} x_c + C_{0d} x_d + u_0, \tag{22}$$

and for each $i = 1, \ldots, m_d$,

$$\dot{x}_i = A_{q_i} x_i + L_{i0} h_0 + L_{id} h_d + B_{q_i}\left[u_i + E_{ia}^- x_a^- + E_{ic} x_c + \sum_{j=1}^{m_d} E_{ij} x_j \right] + E_{di} w, \tag{23}$$

$$h_i = C_{q_i} x_i, \quad h_d = C_d x_d. \tag{24}$$

Here the states x_a^-, x_c and x_d are, respectively, of dimensions n_a^-, n_c and $n_d = \sum_{i=1}^{m_d} q_i$, while x_i is of dimension q_i for each $i = 1, \ldots, m_d$. The control vectors u_0, u_d and u_c are, respectively, of dimensions $m_0 = \operatorname{rank}(D_2)$, m_d and $m_c = m - m_0 - m_d$ while the output vectors h_0 and h_d are, respectively, of dimensions $p_0 = m_0$ and $p_d = m_d$. The matrices A_{q_i}, B_{q_i}, and C_{q_i} have the following form:

$$A_{q_i} = \begin{bmatrix} 0 & I_{q_i - 1} \\ 0 & 0 \end{bmatrix}, \quad B_{q_i} = \begin{bmatrix} 0 \\ 1 \end{bmatrix}, \quad C_{q_i} = [1, 0, \ldots, 0]. \tag{25}$$

Moreover, the eigenvalues of A_{aa}^- are all in the left half complex plane, i.e., they are stable, and the pair (A_{cc}, B_c) is controllable.

Step S.F.2: Let F_c be any arbitrary $m_c \times n_c$ matrix subject to the constraint that

$$A_{cc}^c = A_{cc} - B_c F_c, \tag{26}$$

is a stable matrix.

Step S.F.3: This step makes use of subsystems, $i = 1$ to m_d, represented by (23). Let us choose $\Lambda_i = \{\lambda_{i1}, \lambda_{i2}, \ldots, \lambda_{iq_i}\}$, $i = 1$ to m_d, be the sets of q_i elements all in $\mathbb{C}^-$, which are closed under complex conjugation. Let $\Lambda_d := \Lambda_1 \cup \Lambda_2 \cup \ldots \cup \Lambda_{md}$. For $i = 1$ to m_d, we define

$$p_i(s) := \prod_{j=1}^{q_i} (s - \lambda_{ij}) = s^{q_i} + F_{i1} s^{q_i - 1} + \ldots + F_{iq_i - 1} s + F_{iq_i}, \tag{27}$$

and

$$\tilde{F}_i(\epsilon) := \frac{1}{\epsilon^{q_i}} F_i S_i(\epsilon), \tag{28}$$

where

$$F_i = [F_{iq_i} \;\; F_{iq_i - 1} \;\; \ldots \;\; F_{i1}],$$
$$S_i(\epsilon) = \operatorname{diag}\{1, \epsilon, \epsilon^2, \ldots, \epsilon^{q_i - 1}\}. \tag{29}$$

Step S.F.4: Finally, the parameterized state feedback gain that solves the H_∞-ADDPMS for Σ of (16) is given by as

$$F(\epsilon) := -\Gamma_i \begin{bmatrix} C_{0a}^- & C_{0c} & C_{0d} \\ E_{da}^- & E_{dc} & \tilde{F}_d(\epsilon) + E_d \\ E_{ca}^- & F_c & 0 \end{bmatrix} \Gamma_s^{-1}, \tag{30}$$

where

$$E_d = \begin{bmatrix} E_{11} & \cdots & E_{1m_d} \\ \vdots & \ddots & \vdots \\ E_{m_d 1} & \cdots & E_{m_d m_d} \end{bmatrix}, \tag{31}$$

and

$$\tilde{F}_d(\epsilon) = \operatorname{diag}\{\tilde{F}_1(\epsilon), \tilde{F}_2(\epsilon), \ldots, \tilde{F}_{m_d}(\epsilon)\}. \tag{32}$$

This concludes the ATEA algorithm for the state feedback case.

Stage 2. We now design a reduced order measurement feedback controller that solves the H_∞-ADDPMS for the system (11), in which the subsystem Σ_P is right invertible and of minimum phase, and the subsystem Σ_Q is left invertible and of minimum phase. First, without loss of generality and for simplicity of presentation, we assume that the matrices C_1 and D_1 are already in the form,

$$C_1 = \begin{bmatrix} 0 & C_{1,02} \\ I_k & 0 \end{bmatrix} \quad \text{and} \quad D_1 = \begin{bmatrix} D_{1,0} \\ 0 \end{bmatrix}, \tag{33}$$

where $k = l - \operatorname{rank}(D_1)$ and $D_{1,0}$ is of full rank. Then the given system (11) can be written as

$$\begin{cases} \begin{pmatrix} \dot{x}_1 \\ \dot{x}_2 \end{pmatrix} = \begin{bmatrix} A_{11} & A_{12} \\ A_{21} & A_{22} \end{bmatrix} \begin{pmatrix} x_1 \\ x_2 \end{pmatrix} + \begin{bmatrix} B_1 \\ B_2 \end{bmatrix} u + \begin{bmatrix} E_1 \\ E_2 \end{bmatrix} w, \\ \begin{pmatrix} y_0 \\ y_1 \end{pmatrix} = \begin{bmatrix} 0 & C_{1,02} \\ I_k & 0 \end{bmatrix} \begin{pmatrix} x_1 \\ x_2 \end{pmatrix} + \begin{bmatrix} D_{1,0} \\ 0 \end{bmatrix} w, \\ z = [C_{2,1} \;\; C_{2,2}] \begin{pmatrix} x_1 \\ x_2 \end{pmatrix} + D_2 u, \end{cases} \tag{34}$$

where the original state x is partitioned to two parts, x_1 and x_2; and y is partitioned to y_0 and y_1 with $y_1 \equiv x_1$. Thus, one needs to estimate only the state x_2 in the reduced order controller design. Next, define an auxiliary subsystem Σ_{QR} characterized by a matrix quadruple (A_R, E_R, C_R, D_R), where

$$(A_R, E_R, C_R, D_R) = \left(A_{22}, E_2, \begin{bmatrix} C_{1,02} \\ A_{12} \end{bmatrix}, \begin{bmatrix} D_{1,0} \\ E_1 \end{bmatrix} \right). \tag{35}$$

The following is a step-by-step algorithm that constructs the reduced order output feedback controller for the general H_∞-ADDPMS.

Step R.O.1: Define an auxiliary system

$$\begin{cases} \dot{x} = A \; x + B \; u + E \; w, \\ y = \; x \\ z = C_2 \; x + D_2 \; u, \end{cases} \tag{36}$$

and then perform Steps S.F.1 to S.F.4 of the previous algorithm to the above system to get the parameterized gain matrix $F(\epsilon)$. We let $F_P(\epsilon) = F(\epsilon)$.

Step R.O.2: Define another auxiliary system

$$\begin{cases} \dot{x} = A_R' \; x + C_R' \; u + C_{2,2}' \, w, \\ y = \; x \\ z = E_R' \; x + D_R' \; u, \end{cases} \tag{37}$$

and then perform Steps S.F.1 to S.F.4 of the previous algorithm to the above system to get the parameterized gain matrix $F(\epsilon)$. We let $K_R(\epsilon) = F(\epsilon)'$.

Step R.O.3: Let us partition $F_P(\epsilon)$ and $K_R(\epsilon)$ as,

$$F_P(\epsilon) = [F_{P1}(\epsilon) \quad F_{P2}(\epsilon)] \quad \text{and}$$
$$K_R(\epsilon) = [K_{R0}(\epsilon) \quad K_{R1}(\epsilon)] \tag{38}$$

in conformity with the partition $x = \begin{pmatrix} x_1 \\ x_2 \end{pmatrix}$ and $y = \begin{pmatrix} y_0 \\ y_1 \end{pmatrix}$, respectively. Then define

$$G_R(\epsilon) = [-K_{R0}(\epsilon), \quad A_{21} + K_{R1}(\epsilon)A_{11} - (A_R + K_R(\epsilon)C_R)K_{R1}(\epsilon)]. \tag{39}$$

Finally, the parameterized reduced order output feedback controller is given by

$$\Sigma_{RC}(\epsilon) : \begin{cases} \dot{x}_c = A_{RC}(\epsilon) \quad x_c + B_{RC}(\epsilon) \quad y, \\ u = C_{RC}(\epsilon) \quad x_c + D_{RC}(\epsilon) \quad y, \end{cases} \tag{40}$$

where

$$\left.\begin{aligned} A_{RC}(\epsilon) &:= A_R + B_2F_{P2}(\epsilon) + K_R(\epsilon)C_R + K_{R1}(\epsilon)B_1F_{P2}(\epsilon), \\ B_{RC}(\epsilon) &:= G_R(\epsilon) + [B_2 + K_{R1}(\epsilon)B_1][0, F_{P1}(\epsilon) - F_{P2}(\epsilon)K_{R1}(\epsilon)], \\ C_{RC}(\epsilon) &:= F_{P2}(\epsilon), \\ D_{RC}(\epsilon) &:= [0, F_{P1}(\epsilon) - F_{P2}(\epsilon)K_{R1}(\epsilon)]. \end{aligned}\right\}$$

Now, we are ready to design our gyro-stabilized mirror system. Our goal is to design a simple and low order controller such that the overall system will: (i) have fast tracking in both the yaw and the pitch axes for step input commands (the settling time should not exceed 1 second for a step command with a magnitude up to 10°); (ii) have zero overshoots; (iii) minimize the cross-coupling interactions between the yaw and pitch axes (less than 0.5°); and (iv) ensure that the overall system is robust to external disturbances and changes in system parameters. As will be seen shortly, our controller is very simple and has low order. Thus, it can easily be implemented using low speed personal computers and A/D and D/A cards.

First of all, we need to linearize the dynamical model given in Eqs. (1)–(2) and cast it into the standard state space form. The linearized state space model is given as follows:

$$\dot{x}_g = A_g x_g + B_g u + E_g w_g, \tag{42}$$

where $x_g = (\theta_1, \dot{\theta}_1, \theta_2, \dot{\theta}_2)'$, $u = (u_1, u_2)'$, and $w_g \in \mathcal{L}_2$ is the viscous damping for the system, which can be regarded as disturbances. The matrices A_g, B_g, and E_g are given by

$$A_g = \begin{bmatrix} 0 & 1 & 0 & 0 \\ 0 & 0 & 0 & -\bar{k}\dot{\theta}_3/N_1 \\ 0 & 0 & 0 & 1 \\ 0 & \bar{k}\dot{\theta}_3/N_2 & 0 & 0 \end{bmatrix},$$

$$B_g = \begin{bmatrix} 0 & 0 \\ 1/N_1 & 0 \\ 0 & 0 \\ 0 & 1/N_2 \end{bmatrix}, \quad E_g = \begin{bmatrix} 0 & 0 \\ -1 & 0 \\ 0 & 0 \\ 0 & -1 \end{bmatrix}, \tag{43}$$

where

$$N_1 = \bar{a} + \bar{b} + \frac{\bar{e} + \bar{g}}{2} + \bar{l}, \quad N_2 = \bar{c} + \frac{\bar{f}}{4} + \bar{l}. \tag{44}$$

The measurement output of the free gyro-stabilized mirror system is

$$\theta = \begin{pmatrix} \theta_1 \\ \theta_2 \end{pmatrix}. \tag{45}$$

Since we are interested in the changes in the orientation of the LOS, we focus only on the case where the command input $r(t)$ is a step function. To be more specific, we consider

$$r(t) = \begin{bmatrix} r_1(t) \\ r_2(t) \end{bmatrix} = \begin{bmatrix} \psi_1 \\ \psi_2 \end{bmatrix} 1(t) = \Psi \cdot 1(t), \tag{46}$$

where $1(t)$ is the unit step function, and ψ_1, ψ_2 are some constants. Then, we have

$$\dot{r}(t) = \begin{bmatrix} \dot{r}_1(t) \\ \dot{r}_2(t) \end{bmatrix} = \begin{bmatrix} \psi_1 \\ \psi_2 \end{bmatrix} \delta(t) = \Psi \cdot \delta(t), \tag{47}$$

where $\delta(t)$ is the unit impulse function. Let us define a controlled output h as the difference between the actual output θ and the command input r, i.e.,

$$h = \theta - r = \begin{pmatrix} \theta_1 - r_1 \\ \theta_2 - r_2 \end{pmatrix}. \tag{48}$$

Obviously, h is simply the tracking error. Finally, we obtain the following system in the standard state space form:

$$\Sigma : \begin{cases} \dot{x} = A \quad x + B \quad u + E \quad w, \\ y = C_1 \quad x \quad + D_1 \quad w, \\ h = C_2 \quad x + D_2 \quad u, \end{cases} \tag{49}$$

with

$$x = \begin{pmatrix} \tilde{x}_g \\ r \end{pmatrix} = \begin{pmatrix} \theta_1 \\ \dot{\theta}_1 \\ \theta_2 \\ \dot{\theta}_2 \\ r_1 \\ r_2 \end{pmatrix}, \quad u = \begin{pmatrix} u_1 \\ u_2 \end{pmatrix},$$

$$w = \begin{pmatrix} w_g \\ \delta(t) \end{pmatrix}, \quad y = \begin{pmatrix} \theta_1 \\ \theta_2 \\ r_1 \\ r_2 \end{pmatrix}, \tag{50}$$

$$A = \begin{bmatrix} A_g & 0 \\ 0 & 0 \end{bmatrix}, \quad B = \begin{bmatrix} B_g \\ 0 \end{bmatrix}, \quad E = \begin{bmatrix} E_g & 0 \\ 0 & \Psi \end{bmatrix},$$
$$D_1 = 0, \quad D_2 = 0, \tag{51}$$

and

$$C_1 = \begin{bmatrix} 1 & 0 & 0 & 0 & 0 & 0 \\ 0 & 0 & 1 & 0 & 0 & 0 \\ 0 & 0 & 0 & 0 & 1 & 0 \\ 0 & 0 & 0 & 0 & 0 & 1 \end{bmatrix},$$

$$C_2 = \begin{bmatrix} 1 & 0 & 0 & 0 & -1 & 0 \\ 0 & 0 & 1 & 0 & 0 & -1 \end{bmatrix}. \tag{52}$$

It can be verified that:

1. The subsystem (A, B, C_2, D_2) is invertible with two invariant zeros at 0, which comes from the command input. It also has two infinite zeros of order 2.
2. The subsystem (A, E, C_1, D_1) is left invertible and of minimum phase with no invariant zeros. It has one infinite zero of order 1 and two infinite zeros of order 2.

Utilizing the algorithms of the previous section, which are implemented in a MATLAB toolbox by Chen (1996), we obtained after few iterations the following state feedback gain,

$$F = -\begin{bmatrix} 2.3732 & 1.0271 & 1.4264 & 0.0000 & -2.3732 & -1.4264 \\ -1.4264 & 0.0000 & 2.3732 & 1.0113 & 1.4264 & -2.3732 \end{bmatrix}, \tag{53}$$

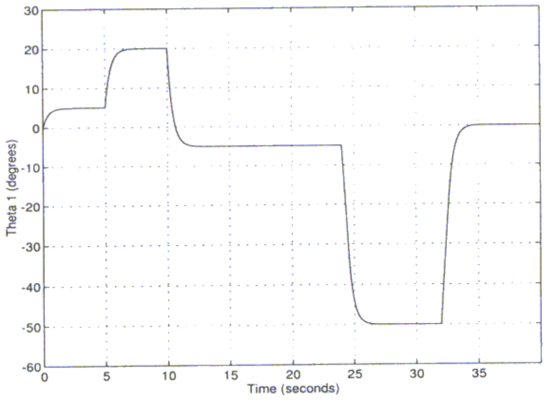

(a) Response for θ_1.

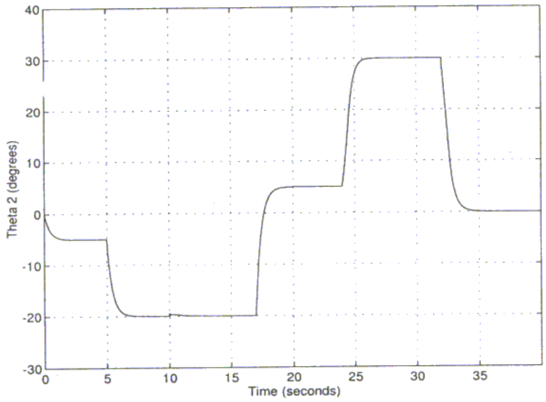

(b) Response for θ_2.

Fig. 2 Simulation result: Responses of θ_1 and θ_2

and the following reduced order observer gain matrix K_R,

$$K_R = -\begin{bmatrix} 85.4439 & 21.2201 & 0 & 0 \\ 21.2201 & 122.3176 & 0 & 0 \end{bmatrix}, \tag{54}$$

which yield a reduced order measurement feedback control law of the form (12) with

$$A_c = \begin{bmatrix} -174.3280 & -74.2370 \\ 106.2743 & -332.7939 \end{bmatrix}, \tag{55}$$

$$B_c = \begin{bmatrix} -83.3798 & -64.5160 & 1.0269 & 0.6172 \\ 11.5772 & -194.7265 & -1.4843 & 2.4695 \end{bmatrix}, \tag{56}$$

$$C_c = \begin{bmatrix} -205.4112 & 0 \\ 0 & -202.2678 \end{bmatrix}, \tag{57}$$

$$D_c = \begin{bmatrix} -90.1288 & -23.2207 & 2.3732 & 1.4264 \\ -20.0343 & -126.0777 & -1.4264 & 2.3732 \end{bmatrix}. \tag{58}$$

As it will be seen in the next section, this controller will produce a satisfactory result.

4 Simulation and Implementation Results

In order to implement our controller designed in the previous section using our hardware setup, we need to discretize it. The performance of this discretized controller is then evaluated using MATLAB Simulink. Finally, it is applied to the actual free gyro-stabilized mirror system. Using the well-known bilinear transformation with a sampling time of 4 ms, we obtained the following discretized controller,

$$\Sigma_d : \begin{cases} v(k+1) = A_d \ \ v(k) + B_d \ \ y(k), \\ u(k) \quad\quad = C_d \ \ v(k) + D_d \ \ y(k), \end{cases} \tag{59}$$

where

$$A_d = \begin{bmatrix} 0.4624 & -0.1304 \\ 0.1866 & 0.1841 \end{bmatrix}, \tag{60}$$

$$B_d = \begin{bmatrix} -61.7225 & -34.4820 & 0.8476 & 0.2904 \\ -0.9257 & -121.3119 & -0.7830 & 1.5197 \end{bmatrix}, \tag{61}$$

$$C_d = \begin{bmatrix} -0.6008 & 0.0536 \\ -0.0755 & -0.4790 \end{bmatrix}, \tag{62}$$

$$D_d = \begin{bmatrix} -64.7719 & -9.0547 & 2.0249 & 1.3072 \\ -19.6598 & -77.0027 & -1.1097 & 1.7584 \end{bmatrix}. \tag{63}$$

The simulation of the overall free gyro-stabilized mirror system is done using the Simulink package of MATLAB. In order to achieve more accurate results, the nonlinear model given in equations (1)–(2) is used. Simulations are carried out using the Runge-Kutta 5 method with both minimum and maximum step sizes set to be the same as the sampling period, i.e., 4 ms. To account for the limitations in the torque motors, a saturation block is added to each of them. The limits are set to be ± 0.5 Nm. Throughout the simulations, the gyro's spin velocity is set to be 2500 rpm.

The gyro is first commanded to move simultaneously to (yaw, pitch) = ($5°$, $-5°$). On the fifth seconds, it is moved from this new

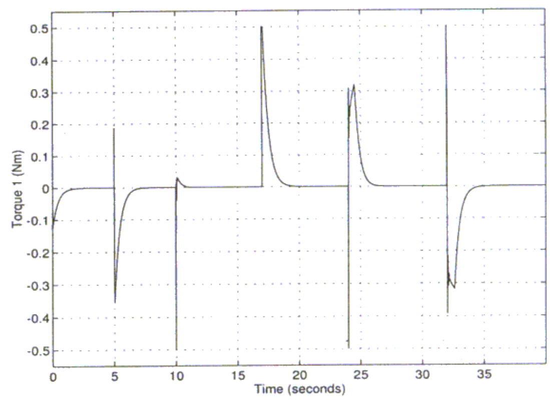

(a) Control input, u_1.

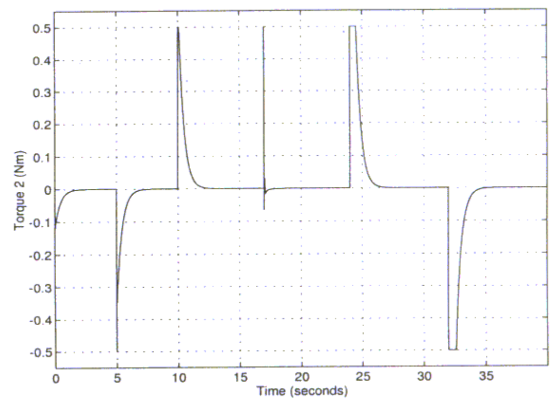

(b) Control input, u_2.

Fig. 3 Simulation result: Control inputs u_1 and u_2

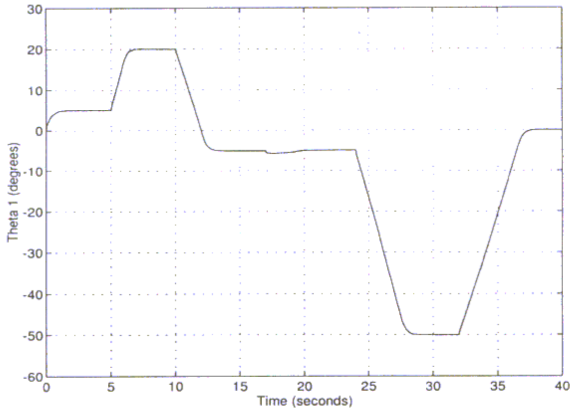

(a) Response for θ_1.

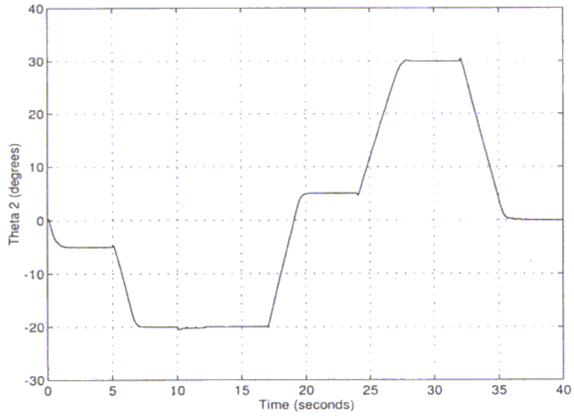

(b) Response for θ_2.

Fig. 4 Implementation with dead zone compensation: θ_1 and θ_2

position to (20°, −20°). A horizontal span is then carried out, i.e., the gyro is moved horizontally from 20° to −5° while keeping the pitch position at −20°. This is followed by a vertical span; this time the yaw position is fixed at −5° while the pitch position is changed from −20° to 5°. Finally, it is pushed to its extreme position (−50°, 30°) before returning back to its zero position. The gyro's response as well as the torque input to each axis are plotted in Figs. 2–3.

The various set-points in the above tests are chosen such that from one position to another, the displacement ranges from as small as 5° up to 45°. This is to verify that our controller works well within the whole workspace although it is designed based on a linearized model. The simultaneous movement is to test whether our controller is capable of achieving perfect tracking in both axes while the spans are conducted to investigate how well does our controller 'decouple' the gyro-stabilized mirror system. As can be seen from the responses in Fig. 2, the gyro is able to reach all commanded positions without steady state errors. Furthermore, none of the responses exhibits any overshoot. The settling time from its extreme position back to the zero position is about 3.5 seconds. The maximum coupled movement in θ_1 caused by moving θ_2 is around 0.15°. The maximum coupled movement in θ_2 caused by moving θ_1 is about 0.5°. A check with Fig. 3 shows that all these are accomplished with the torques kept within the constraint of ±0.5 Nm. Thus we conclude that our controller designed in the previous section is very satisfactory.

Next, we implement this controller on the actual free gyro-stabilized mirror system via a computer and perform the whole test once again. During implementation process, we observe that there are dead zones in both torque motors, which cause steady-state errors in the both axes. Through trial and error, we find that the magnitude of the dead zone compensation seems to be related to the set-points in the following way:

$$u_{os1} = \alpha_1 r_1 + \beta_1 r_2 \quad \text{and} \quad u_{os2} = \alpha_2 r_1 + \beta_2 r_2, \tag{64}$$

where u_{os1} and u_{os2} are the values to be added to u_1 and u_2, respectively. Various sets of (r_1, r_2) are used to tune α_1, α_2, β_1 and β_2 so as to obtain suitable offsets to be added to the control inputs such that the dead zone effects can be minimized. Figures 4 and 5 are the results we obtain from our controller with a dead zone compensation whose parameters are chosen as follows:

$$\alpha_1 = -0.001125, \quad \beta_1 = -0.000125,$$

$$\alpha_2 = -0.0049875, \quad \beta_2 = -0.00059375. \tag{65}$$

The results show that our controller is able to perform fast tracking without overshoots in the both axes and minimize the coupled effect (0.8° in the yaw axis and 0.5° in the pitch axis) on the actual system. In fact, the actual performance of our controller matches quite well with the simulation results given in Fig. 2. All the design specifications are fully achieved.

In order to test the robustness of this controller, we send a command to move the gyro simultaneously in the yaw (+20°) and pitch (−20°) direction. Then we purposely introduce some disturbance (through knocking on the gimbals) to the system. As shown in Fig. 6, our controller is robust to this external disturbance.

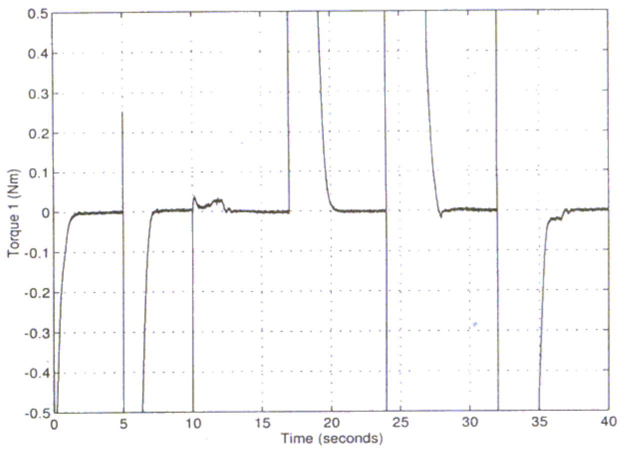

(a) Control input, u_1.

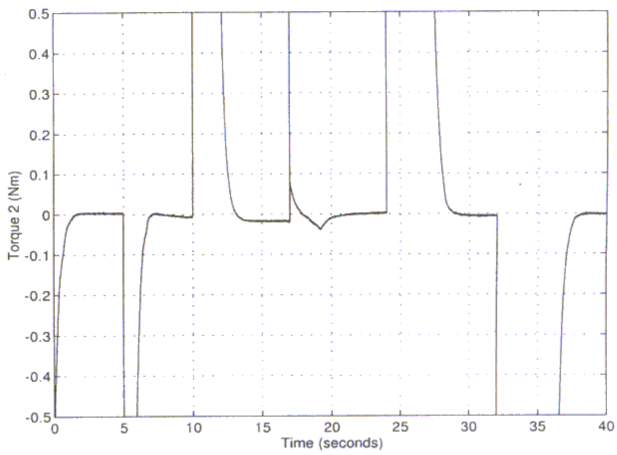

(b) Control input, u_2.

Fig. 5 Implementation with dead zone compensation: u_1 and u_2

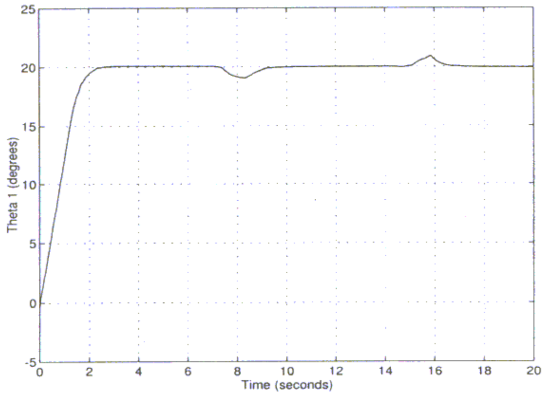

(a) Response for θ_1.

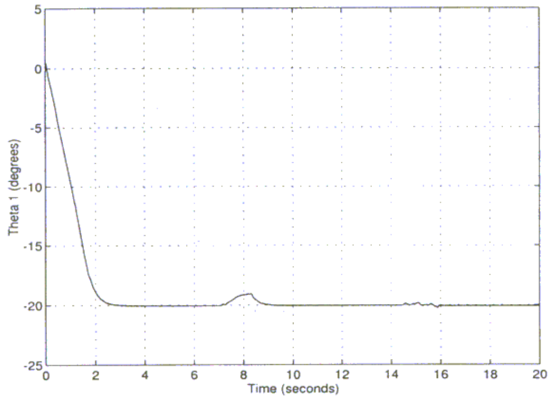

(b) Response for θ_2.

Fig. 6 Robustness test for the final system

5 Conclusions

In this paper, we have designed and implemented a measurement feedback controller for a multivariable servomechanism gyro-stabilized mirror system. We first formulated the design into an H_∞ control problem and then applied the asymptotic time-scale and eigenstructure method of Chen et al. (1998) to solve the problem. Both simulation and implementation studies show that our design is very successful. Finally, we note that controllers obtained using other techniques such as adaptive feedforward control in Lee et al. (1996), neural network control in Ge et al. (1997) and fuzzy logic in Lee (1995), are generally too complicated to be implemented in the real system with a slow personal computer.

Acknowledgment

The authors would like to thank the anonymous reviewers for their constructive comments that improved the presentation of this paper. Special thanks to one of the reviewers in particular for his or her help in correcting grammatical errors and styles in the original draft.

References

Bigley, W. J., and Rizzo, V. J., 1987, "Wideband Linear Quadratic Control of a Gyro Stabilized Electro-Optical Sight System," *IEEE Control Systems Magazine,* Vol. 7, pp. 20–24.

Chen, B. M., 1996, *Linear Systems and Control Toolbox,* Technical Report, Department of Electrical Engineering, National University of Singapore, Singapore.

Chen, B. M., 1998, *H_∞ Control and Its Applications,* Springer, New York.

Chen, B. M., Lin, Z., and Hang, C. C., 1998, "Solutions to General H_∞ Almost Disturbance Decoupling Problem with Measurement Feedback and Internal Stability," *International Journal of Control,* Vol. 71, No. 4, pp. 653–685.

Constancis, P., and Sorine, M., 1992, "Wide-Band Control of Gyro Accelerometer Multisensors in a Strapdown Guidance-System," *Journal of Guidance Control and Dynamics,* Vol. 15, No. 4, pp. 855–860.

Dzielski, J., Bergmann, E., Paradiso, J. A., Rowell, D., and Wormley, D., 1991, "Approach to Control Moment Gyroscope Steering Using Feedback Linearization," *Journal of Guidance Control and Dynamics,* Vol. 14, No. 1, pp. 96–106.

Ge, S. S., Lee, T. H., and Zhao, Q., 1997, "Real-Time Neural Network Control of a Free Gyro-Stabilized Mirror," *Proceedings of the 1997 American Control Conference,* Albuquerque, NM, pp. 1076–1080.

Lee, T. H., Koh, E. K., and Loh, M. K., 1996, "Stable Adaptive Control of Multivariable Servomechanisms, with Application to a Passive Line-of-Sight Stabilization System," *IEEE Transactions on Industrial Electronics,* Vol. 43, No. 1, pp. 98–105.

Lee, M. W., 1995, *An Investigation in Fuzzy Logic,* B.Eng. thesis, Department of Electrical Engineering, National University of Singapore.

Ng, W. K., 1986, *Design Considerations of a Gyro-Stabilized Mirror System,* B.Eng. thesis, Department of Electrical Engineering, National University of Singapore.

Perry, J., 1957, *Spinning Tops and Gyroscopic Motion,* Dover Publications, New York.

Saberi, A., and Sannuti, P., 1990, "Squaring Down of Non-Strictly Proper Systems," *International Journal of Control,* Vol. 51, pp. 621–629.

Sannuti, P., and Saberi, A., 1987, "A Special Coordinate Basis of Multivariable Linear Systems—Finite and Infinite Zero Structure, Squaring Down and Decoupling," *International Journal of Control,* Vol. 45, pp. 1655–1704.

Yang, L. F., and Chang, W. H., 1996, "Synchronization of Twin-Gyro Precession Under Cross-Coupled Adaptive Feedforward Control," *Journal of Guidance Control and Dynamics,* Vol. 19, No. 3, 534–539.